Available online at www.sciencedirect.com
ScienceDirect
Journal of the European Ceramic Society 31 (2011) 1661–1667
www.elsevier.com/locate/jeurceramsoc

Fabrication and characterization of composite sol–gel coatings on porous ceramic substrate

M. Touzin *, F. Béclin

Unité Matériaux et Transformations, UMR CNRS 8207, Université de Lille 1, 59655 Villeneuve d'Ascq, France

Received 22 September 2010; received in revised form 18 February 2011; accepted 1 March 2011
Available online 5 April 2011

Abstract

Highly porous ceramic materials were coated using a composite sol–gel method. Alumina powder is dispersed in a silica sol–gel solution and then dip-coated on the substrate. The resulting coatings present a composite microstructure in which crystalline alumina grains are linked to each other by an amorphous silica phase. In this work, we show that, by accurately controlling the sol–gel parameters (water, solvent and silica precursor (TEOS) ratio, pH and ageing time of the sol) and also the powder grain size distribution it is possible to obtain crack-free thick films (more than 20 μm in one step). These coatings present good adherence to the substrate, decrease the roughness and also close the surface porosity of the substrate. Coating mechanical properties have been evaluated thanks to micro-indentation measurements and linked to coating structural evolution with the thermal treatment temperature.

Keywords: Films; Sol–gel processes; Composites; Mechanical properties; Al_2O_3

1. Introduction

Porous ceramic materials are widely used in several application domains including construction materials, filters, electronics sensors, catalysts, heat insulators.[1–3] Indeed, these materials present a lot of interesting properties such as lightness, thermal insulation, thermal shock resistance or high specific surface area. This kind of materials often exhibits open porosity and high roughness that is necessary for some applications such as filtration or catalyst but could be not compatible with some others. In these latter cases, it is then necessary to modify the surface of such materials by closing the surface porosity and reducing the surface roughness. This surface modification can be obtained by coating. Sol–gel process is an important technique for producing high quality glasses and fine ceramics, and especially for synthetizing coatings. Producing coatings by this way presents a lot of advantages such as low temperature, cost effectiveness and the possibility of coating different substrate materials and complex geometries. However, an important limitation of this process is that the thickness of the coatings is limited to less than 1 μm because of the stresses induced by drying and densification processes of the gel, leading to the cracking of the film. In order to obtain much thicker crack-free films, the classical sol–gel method can be modified by incorporating in the sol a ceramic powder.[4–7] In that case, the gel phase plays the role of a strong binder between the ceramic grains, making it less likely that the film will crack during processing. Moreover, due to the great amount of ceramic powder, the amount of sol–gel in the film is decreased and less shrinkage occurs when the film is processed. The coatings obtained by this method present thickness that can be greater than 50 μm without any crack. In this paper, we describe the processing and the microstructural characterization of sol–gel composite (Al_2O_3/SiO_2) coatings deposited on highly porous ceramic substrates in order to close the open porosity and to make the surface smoother. Micro-hardness is measured and correlated to the processing variables of the coatings. Moreover, micro-indentation measurements are used as a tool to obtain information on coating structure.

* Corresponding author. Tel.: +33 3 20 43 65 94; fax: +33 3 20 43 65 91.
E-mail addresses: matthieu.touzin@univ-lille1.fr (M. Touzin), franck.beclin@univ-lille1.fr (F. Béclin).

0955-2219/$ – see front matter © 2011 Elsevier Ltd. All rights reserved.
doi:10.1016/j.jeurceramsoc.2011.03.002

Table 1
Grain size characteristics of alumina powders used for coating processing (data from Alcoa society).

Alumina powder	d_{50} (μm)	d_{90} (μm)
A	0.3	0.7
B	1.0–1.4	2.0–3.5
C	3.5–5.0	9.0–15.0

2. Experimental procedure

2.1. Thick film fabrication

The substrates used in this study are aluminosilicate ceramic materials with 30% of essentially open porosity resulting in a very important surface roughness. The pore size distribution is centered around 50 μm but some pores can reach 100 μm in diameter. Subtrates are mostly composed of mullite and a small amount of partially crystallized silica (in cristobalite form) is also present. Before surface treatment, they were first cleaned ultrasonically in ethanol for 5 min and then in distilled water for 5 min. The thick films were prepared by dispersing alumina powder in a silica sol–gel solution. The resulting suspension was then deposited on a highly porous ceramic substrate by dip-coating. The reagents were used in as-received condition. The silica sol was prepared by mixing tetraethylorthosilicate ($Si(OEt)_4$; TEOS; 98%; Acros Organics, Belgium) with ethanol. Different TEOS/Ethanol molar ratios were studied (1/4, 1/6, 1/8 and 1/10). TEOS was then hydrolyzed by distilled water (TEOS/H_2O/: 1/4) and the resulting sol was magnetically stirred for 30 min. To catalyze hydrolysis and condensation reactions, pH sol was adjusted at a value slightly lower than 2 (∼1.80) by adding hydrochloric acid (HCl, 1 M). Acid catalysis conditions favour long Si–O–Si chain formation and therefore promote film production.[8,9] Furthermore, such a low pH prevents fast gelation of the sol, thus giving time for the powder dispersion.[9] Various grain size commercial calcined α-alumina powders were added to the silica sol (Alcoa, see characteristics in Table 1).

The amount of powder dispersed in the sol represented 50 wt.% of the total mixture. The pH was again adjusted in order to provide good dispersion of alumina powder in the sol and then to obtain a stable suspension. The suspension was stirred for 24 h in order to achieve the powder dispersion. Coatings were obtained by dipping the substrates in the slurry. The withdrawal rates were 1 and 5 mm/s. After drying at 100 °C for 1 h, samples were heat treated at various temperatures (from 600 up to 1400 °C) for 15 min in air at a heating and cooling rate of 2 °C/min. Coating thickness was increased by repeating the whole coating procedure several times (from 1 to 3). Fig. 1 illustrates the preparation process of the coatings.

2.2. Thick film characterization

The coating microstructure and surface topography were examined by transmission electron microscopy (TEM, FEI Tecnai 20 G2) and scanning electron microscopy (SEM, HITACHI S4700). Coating thickness was evaluated on cross-section by SEM. Thin foils used for TEM observations were prepared from slices by mechanically polishing to 30 μm thickness, followed by argon ion milling. A thin film of carbon was deposited on to the foil before examination. X-ray diffraction (XRD) analysis was performed in order to check if any phase transformation occurred during heat treatment. Philips equipment was used for collecting X-ray diffraction data. The Co Kα lines were used as a source. Coating mechanical properties were evaluated by measuring the Vickers micro-hardness on cross-sections mechanically polished with decreasing grain-size abrasive paper and finally finished with a 0.25-μm diamond paste. Instrumented micro-indentation Hardness was measured using Micro Hardness Tester (MHT, CSM instruments, Switzerland) equipped with a Vickers diamond indenter. Indentations have been performed at a load of 500 mN with a loading rate of 1000 mN/min and a dwell of 15 s at maximum load. The load was released at the same rate. For each tested sample, at least 15 different indentations were performed and the mean hardness value was calculated. If a measurement did significantly differ from the average it was excluded and a new test was performed. The hardness results were obtained after numerical treatment of the load/depth curves using the Oliver and Pharr method.[10]

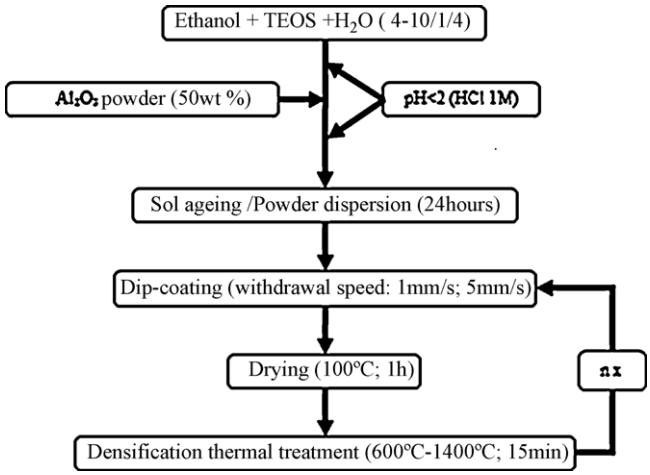

Fig. 1. Flow chart for the preparation of alumina/silica composite coatings.

3. Results and discussion

3.1. How to prevent cracking?

As well known, the cracking of sol–gel coatings during processing constitutes a critical point. So, in order to prepare crack-free coatings, the relationships between different processing parameters and cracking have been studied. Our attention has particularly been focused on the following two parameters: the alumina powder size and the ethanol concentration in the sol. Fig. 2 shows the surface topology of three coatings after a heat treatment performed at 1000 °C for 15 min. It is important to note that the only parameter to differ between these three samples is the grain size of the used alumina powder. As it can be seen, the mean alumina grain size has a great influence on the composite coating cracking. Indeed, coatings synthetized with very

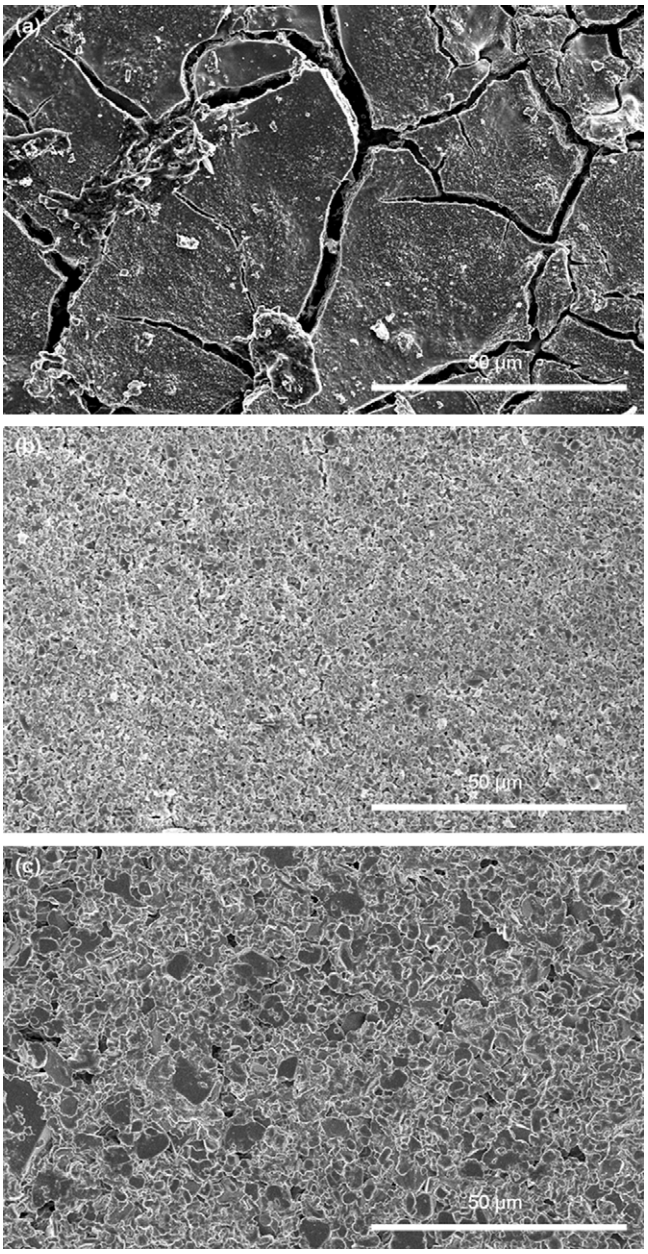

Fig. 2. influence of the alumina grain mean size d on the coating cracking: (a) $d = 0.3$ µm; (b) $d = 1$–1.4 µm; (c) $d = 3$–5 µm; the other processing parameters are the same for the three coatings: water/TEOS/ethanol: 4/1/4; withdrawal speed: 5 mm/s; annealing temperature: 1000 °C.

fine alumina powder ($d = 0.3$ µm; Fig. 2(a)) present a network of big cracks of several tens of micrometers whereas films prepared with coarser powders ($d = 1$–1.4 and 3–3.5 µm; Fig. 2(b) and (c), respectively) do not present such a cracking. It has been noticed that these cracks appeared during the drying treatment at 100 °C and persist after the high temperature treatment at 1000 °C. An interpretation concerning the influence of the powder grain size on the cracking is given by Olding et al.[4]: one of the factors contributing to the cracking is related to residual organics in the coating during the firing process. The use of fine powders in composite sol–gel coatings processing leads to denser materials with smaller pores than those fabricated with coarser powders.

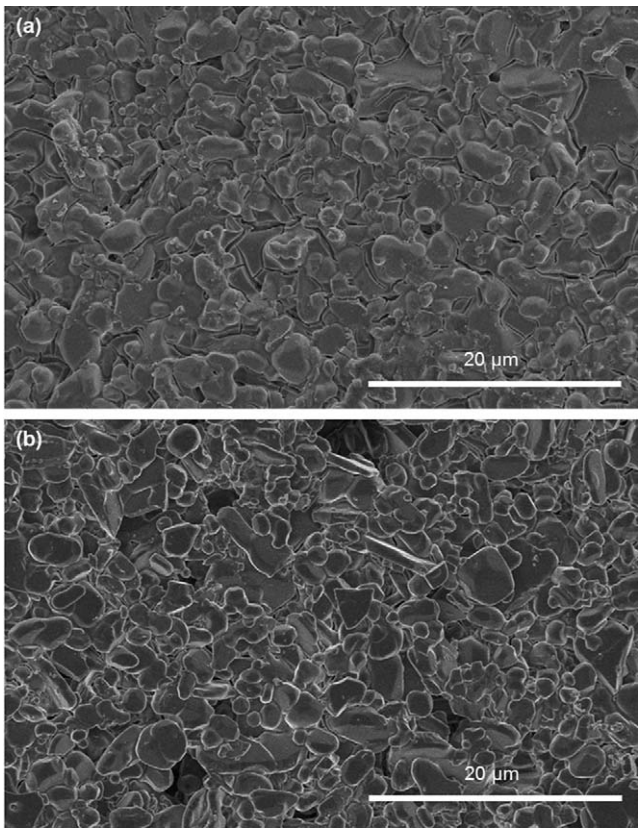

Fig. 3. influence of the ratio water/TEOS/ethanol on the silica matrix cracking (a): 4/1/4; (b) 4/1/10; the other processing parameters are the same for both coatings: alumina mean grain size $d = 3$–5 µm; withdrawal speed: 5 mm/s; annealing temperature: 1000 °C.

The removal of organics from composite coatings is then more difficult in the case of formulations based on small particle size powders. This kind of coating is then much more susceptible to cracking.

As shown in Fig. 3(a), after the densification thermal treatment, samples produced from the coarsest powder ($d = 3$–3.5 µm) present another kind of cracking. These cracks are very different from those discussed previously since they are not greater than few micrometers and located in the amorphous silica phase. For a given powder/sol ratio (in this work: 50 wt.%), the powder grain size increase leads to the increase of the silica layer thickness located between alumina grains. That leads to an increase of the densification stresses and thus induces the cracking of the silica. By decreasing the TEOS/ethanol ration (from 1/4 to 1/10), the silica network becomes more flexible and better accommodates the densification stresses. Thus, as shown in Fig. 3(b), the cracking is avoided even for the coarsest powder.

Taking into account these results, to prevent the coating cracking, two precautions must be respected: the first one is to use a ceramic powder presenting a reasonable mean grain size and the second one is to synthesize a silica gel not too dense. In this work, we have decided to use the alumina powder with mean grain size of 1–1.4 µm and to set the water/TEOS/ethanol ratio equal to 4/1/6 in order to obtain crack-free coatings. The further study has been then performed on these materials.

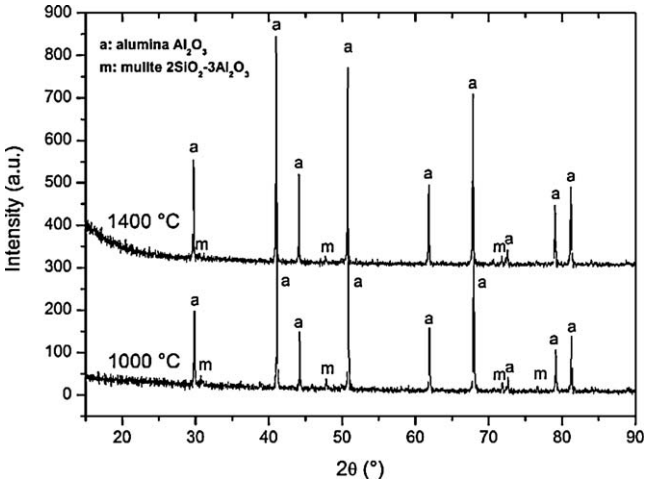

Fig. 4. XRD patterns of coatings heat-treated at 1000 and 1400 °C respectively (mean alumina grain size: 1–1.4 μm; water/TEOS/ethanol: 1/4/6; withdrawal speed: 5 mm/s; 3 layers).

3.2. Coating observation

Fig. 4 shows XRD patterns of two coatings heat-treated at 1000 and 1400 °C, respectively. According to Fig. 4, coatings are composed by crystalline α-alumina and amorphous silica. Some little peaks corresponding to the mullite phase are present in both diagrams. It is assumed that these peaks can be attributed to the substrate. That is confirmed by the fact that the mullite amount does not evolve between 1000 and 1400 °C.

Fig. 5 presents a view of the typical morphology of coatings producted by the "composite sol–gel" process. This picture indicates that the thickness of this coating is about 40–50 μm depending on the substrate roughness. It is interesting to note that the high substrate roughness is attenuated by the coating as well as the presence of the composite film leads to the closure of the surface porosity.

Fig. 6 shows SEM (a) and TEM (b) observations of sol–gel composite coatings. The coatings exhibit a composite microstructure that can be described as crystalline alumina grains embedded in an amorphous silica matrix. Because of the

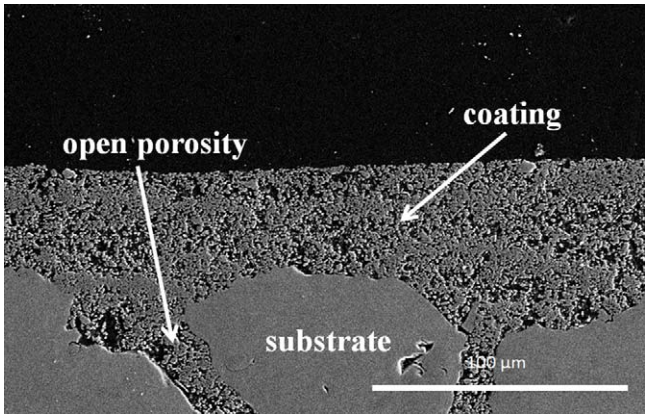

Fig. 5. SEM observation of a composite sol–gel coating – water/TEOS/ethanol: 4/1/6; alumina mean grain size: 1–1.4 μm; withdrawal speed: 5 mm/s; annealing temperature: 1000 °C; 3 layers.

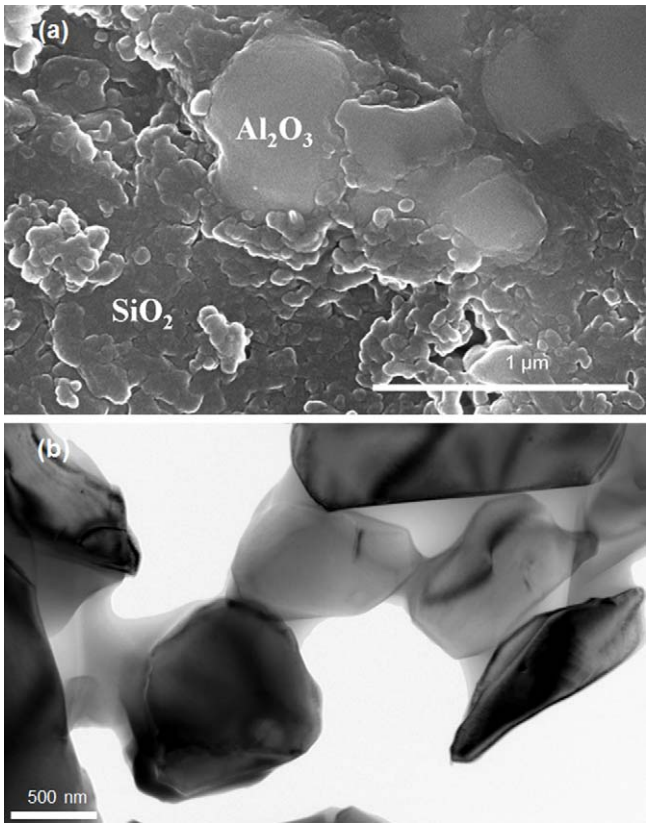

Fig. 6. SEM (a) and TEM (b) Observation of a composite sol–gel coating – water/TEOS/ethanol: 4/1/6; alumina mean grain size: 1–1.4 μm; withdrawal speed: 5 mm/s; annealing temperature: 1000 °C; 3 layers.

silica formation by hydrolysed TEOS molecules condensation into domains, this phase has the appearance of small interconnected nodules of about 100 nm diameter. The alumina grains are well dispersed in the silica phase which plays the role of binder between the grains. It can also been noticed that alumina grains present a good wettability by the silica phase and no porosity is observed between alumina grains and the silica layer. Surface hydroxyl groups which are present on the surface of ceramic powders should react with those present in the silica gel leading to the formation of strong Al–O–Si bonds, thus a good cohesion between grains and amorphous phase is expected. Moreover, after a heat treatment at 1000 °C, coatings exhibit some residual porosity.

Fig. 7 shows the interface between the composite coating and the porous substrate. As it is seen in Fig. 7(a), a layer of sol–gel silica is observable at the interface between the substrate and the coating and thus provides to the latter a good adhesion to the substrate. Indeed, the sol–gel film adheres strongly to the substrate because of the presence of hydroxyl groups on the surface of the oxide constituting the substrate. This very good cohesion of the interface is confirmed by Fig. 7(b). Several indentation prints have been carried out with a load of 1 N exactly at the interface substrate/coating and as it can be seen in the picture, there is no propagation of any crack along the interface.

To improve the surface, in terms of surface porosity closing and surface smoothing, of such porous and rough materials,

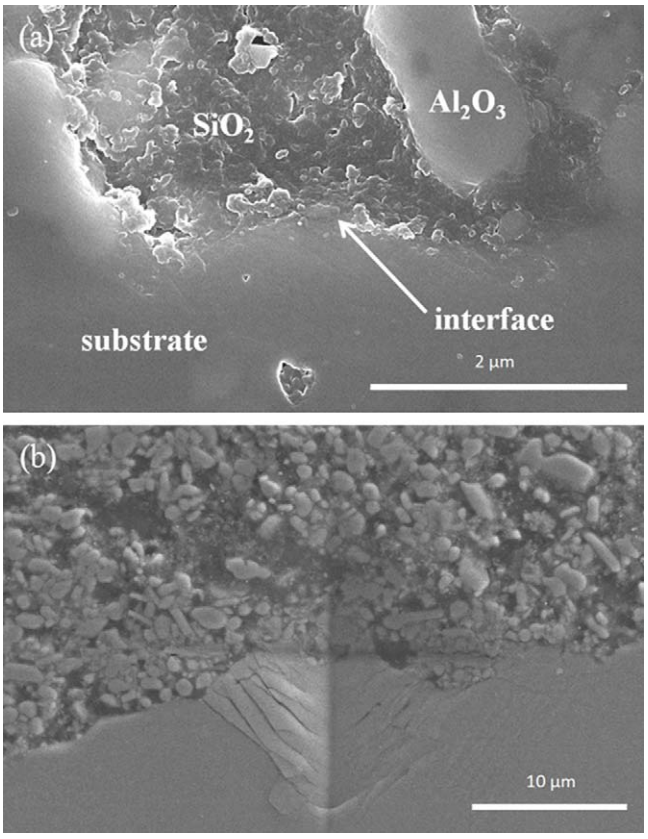

Fig. 7. (a) Sol–gel silica layer at the interface between the substrate and the coating. (b) Indentation print at 1 N load, no crack propagation along the interface is observed.

it is necessary to deposit thick films. It is well known that the coating thickness can be easily controlled by two processing parameters which are the dip-coating withdrawal speed and of course the number of coated layers. The higher the withdrawal speed, the higher the sol dynamic viscosity and consecutively the thicker the deposited film.[11] It is also possible to modify the coating thickness by making variations in other processing parameters such as the sol composition, the ceramic powder amount or the sol ageing time since they all have an influence on the viscosity of the sol and then on the thickness. However, as said previously these parameters have been chosen to prepare crack-free coatings, so we decided to control the coating thickness only by playing on the withdrawal speed and the number of layers. Fig. 8 shows the evolution of the surface topology as a function of the coating thickness. Fig. 8(a) shows the surface of the substrate without any coating, surface pores are numerous. When this substrate is coated by a sol–gel composite film of ~10 µm thick (Fig. 8(b)), the surface porosity decreases but still remains. The withdrawal speed increase (from 1 to 5 mm/s) leads to the thickness increase (~30 µm) and the surface state is really improved (Fig. 8(c)). Almost all the porosity is closed (Fig. 8(d)) by increasing again the film thickness (~80 µm) by depositing two layers.

3.3. Mechanical properties (micro-hardness and creep behaviour)

Mechanical properties of the coatings at room temperature were evaluated by means of micro-indentation measurements. Because of the very high surface roughness of the substrate and to ensure to characterize only coating properties, tests were performed on coated material polished cross-sections. By this ways, we can assume that the substrate doesn't play any role in the material response. Moreover, the diagonal size of the indent print is greater than 10 µm (Fig. 9) that is much larger than the mean grain size, thus many grains are solicited during the measurement and one can consider that results are representative of the global material microstructure. It is also useful to note that

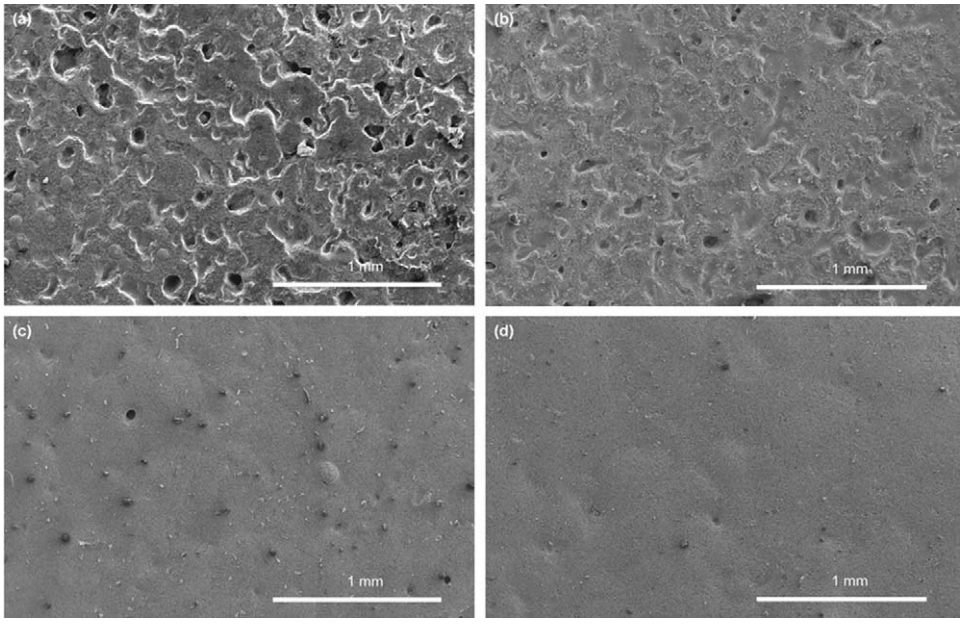

Fig. 8. SEM observation of surface morphology (a) without coating; (b) withdrawal speed: 1 mm/s; 1 layer; (c) withdrawal speed: 5 mm/s; 1 layer; (d) withdrawal speed: 5 mm/s; 2 layers.

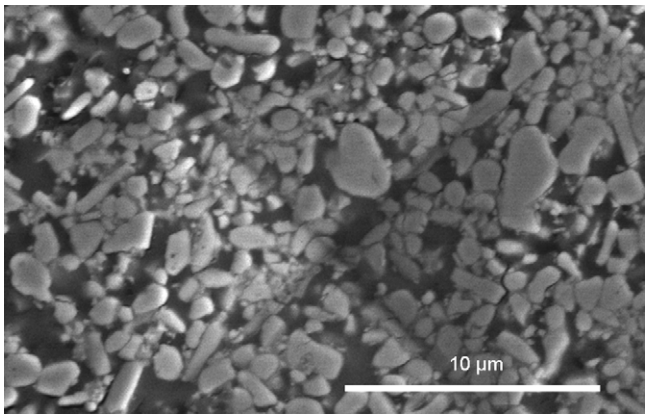

Fig. 9. Typical view of an indent print, showing that numerous grains are solicited and no cracks are created.

the position of the imprint within the coating (i.e. close to the surface or to the substrate) has no significant influence on the result.

Fig. 10 shows typical Vickers indentation responses for composite coatings heat-treated at five different temperatures (from 600 up to 1400 °C, the other processing parameters are the same for all the coatings: water/TEOS/ethanol: 4/1/6; alumina mean grain size: 1–1.4 μm; withdrawal speed: 5 mm/s; 3 layers). The load–displacement curves can be divided, depending on the annealing temperature, in three domains in terms of maximum depth reached by the indent tip at the same load. The maximum depth is four times greater for the coating treated at 600 °C than for the one corresponding to the material heated at 1400 °C. The three other materials (treated at 800, 1000 and 1200 °C) exhibit an intermediate behaviour with a maximum depth only two times greater than the one heated at 1400 °C. It also can be noticed that for all the materials, the deformation rate is not equal to zero when the maximum load is maintained. This deformation under a constant load also seems to strongly depend on the temperature.

The indent penetration depth at maximum load (500 mN) as a function of the time for five treatment temperatures is reported

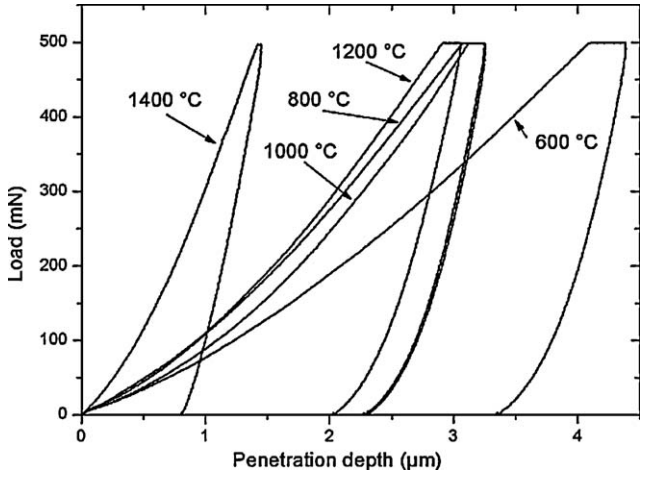

Fig. 10. Indentation load–displacement curves for Vickers indentation – maximum load $P_{max} = 500$ mN (mean alumina grain size: 1–1.4 μm; water/TEOS/ethanol: 1/4/6; withdrawal speed: 5 mm/s; 3 layers).

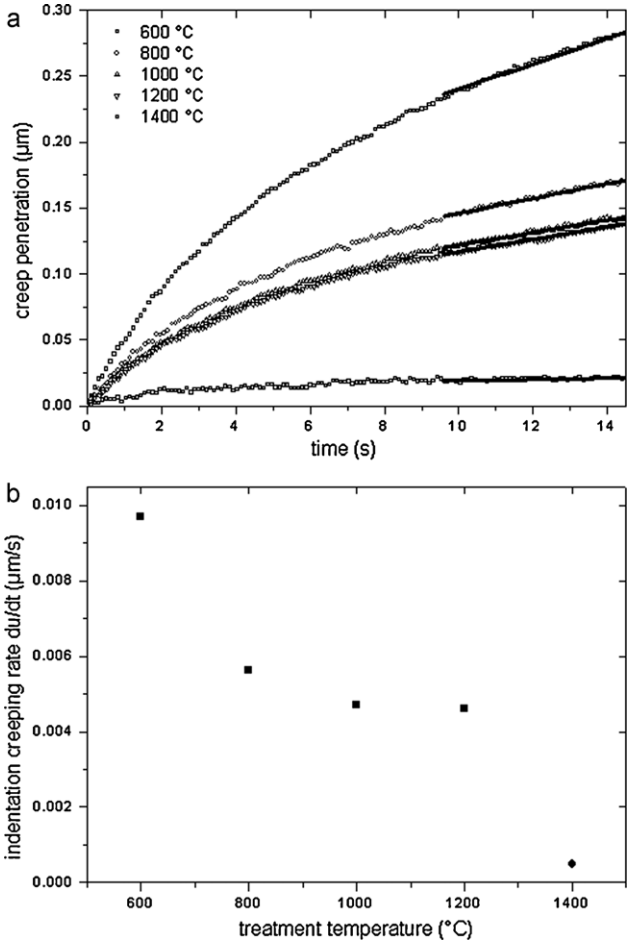

Fig. 11. influence of the densification treatment temperature on the creep behaviour at maximum load 500 mN (mean alumina grain size: 1–1.4 μm; water/TEOS/ethanol: 1/4/6; withdrawal speed: 5 mm/s; 3 layers).

in Fig. 11(a). The duration of maximum load application is very short (15 s), thus the permanent creep regime is not reached and no quantitative analysis can be performed to determine mechanical properties such as viscosity. However, a qualitative analysis is still possible and allows discriminating the different materials depending on their treatment temperature. For that, a pseudo indentation creeping rate has been estimated for each treatment temperature by calculating the slope of the end of each curve (from 10 to 15 s) that can be approximated as a straight line. Indentation creeping rate values as a function of the treatment temperature are reported in Fig. 11(b). Between 600 and 1200 °C, the indentation creeping rate progressively decreases and seems to follow an exponential law. Between 1200 and 1400 °C, this evolution is broken and we observe an abrupt diminution of the creeping rate that adopts a very low value. So this plot seems to indicate that the evolution of the mechanical properties as a function of the treatment temperature can be divided into two domains, not three as said previously.

Fig. 12 shows Vickers microhardness values and average coating thickness as a function of the thermal treatment temperature. Coatings exhibit very low Vickers microhardness values (lower than 300 Hv) for densification temperature up to 1200 °C and a huge increase at 1400 °C (∼1300 Hv). The coating thick-

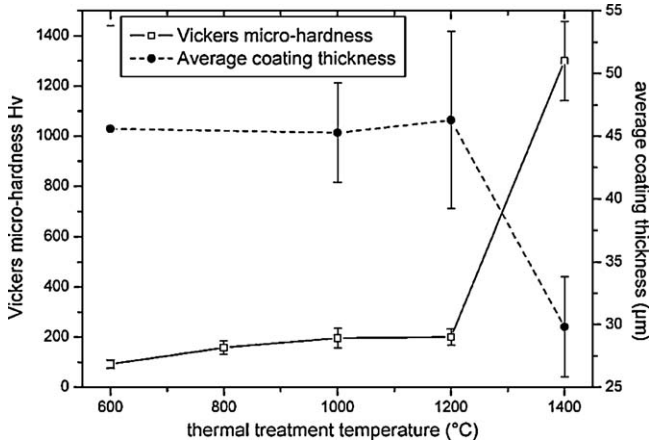

Fig. 12. Vickers micro-hardness and average coating thickness as a function of the densification treatment temperature (mean alumina grain size: 1–1.4 μm; water/TEOS/ethanol: 1/4/6; withdrawal speed: 5 mm/s; 3 layers).

ness evolution presents a plateau between 600 and 1200 °C and then an abrupt decrease at 1400 °C.

These micro-indentation measurements give information on the structure of the composite coatings. According to load–depth curves (Fig. 10) and indentation creep measurements (Fig. 11), coatings seem to present two kinds of behaviour that can be connected to their structure depending on the thermal treatment temperature. Very low micro-hardness value associated to high creeping rate observed for the lowest treatment temperature (600 °C) indicates that the silica phase, which has been synthetized by sol–gel process, presents a typical low density structure of a gel. At higher temperature (from 800 to 1200 °C), the creeping rate decrease points out a change in the silica phase structure. Thanks to thermally activated mechanisms, condensation reactions lead to the increase of the silica gel network connectivity. The gel becomes more and more reticulated and finally turns into glass.[9,12] For these temperatures, the increase of hardness is very weak, denoting that the coatings are still very porous. At 1400 °C, the low creeping rate associated to high micro-hardness values points out a great change in the coating structure. Indeed, it is reasonable to make the assumption that the glass transition temperature T_g takes place between 1200 and 1400 °C. So, at 1400 °C, the viscous flux of the silica glass permits the alumina grains rearrangement and consequently the achievement of the coating densification. This is confirmed by Fig. 11 that shows a huge shrinkage of the coating at 1400 °C. Moreover, XRD patterns of coatings heat-treated at 1000 and 1400 °C indicate that this hardness increase cannot be explained by any phase transformation (see Section 3.2). Micro-hardness of coatings treated at 1400 °C is 1300 Hv that is located just between those of dense alumina (1519 ± 31 Hv[13]) and fused silica (∼900 Hv[14]) and is then compatible with a dense composite of these two phases.

4. Conclusion

Al_2O_3/SiO_2 Composite sol–gel thick coatings were fabricated in order to improve the surface of highly porous ceramic materials. These coatings were prepared by dispersing an alumina powder in silica sol–gel solution and then deposited on the substrate by dipping. Processing parameters were optimized to obtain crack-free thick coatings of more than 50 μm thick. Particular attention has been given to cracking phenomenon and it has been shown that by controlling the powder size and the sol–gel composition, it is possible to drastically diminish it. Resulting coatings exhibit a composite microstructure that consists in crystalline alumina grains linked by an amorphous silica matrix. Moreover, the silica matrix provides to the coating good cohesion to the substrate. As a result, the coatings lead to real improvement of the substrates by closing the open porosity and drastically reducing their roughness. Coating micro-hardness and creeping behaviour were studied by micro-indentation measurements. It was shown that this property is essentially controlled by the silica phase structure that greatly depends on the densification treatment temperature. Micro-indentation measurement provides then an efficien tool for the following of the coating densification.

Acknowledgments

The Conseil Regional du Nord-Pas de Calais and the European Regional Development Fund (ERDF) are acknowledged for the support of this study through the competitiveness cluster MAUD, and also for the support of the SEM and TEM national facility in Lille (France).

References

1. Galassi C. Processing of porous ceramics: piezoelectric materials. *J Eur Ceram Soc* 2006;**26**:2951–8.
2. Kritikaki A, Tsetsekou A. Fabrication of porous alumina ceramics from powder mixtures with sol–gel derived nanometer alumina: effect of mixing method. *J Eur Ceram Soc* 2009;**29**:1603–11.
3. Deng ZY, Fukasawa T, Ando M, Zhang GJ, Ohji T. High-surface-area alumina ceramics fabricated by the decomposition of $Al(OH)_3$. *J Am Ceram Soc* 2001;**84**:485–91.
4. Olding T, Sayer M, Barrow D. Ceramic sol–gel composite coatings for electrical insulation. *Thin Solid Films* 2001;**398–399**:581–6.
5. Barrow DA, Petroff TE, Sayer M. Thick ceramic coatings using a sol gel based ceramic-ceramic 0-3 composite. *Surf Coat Technol* 1995;**76–77**:113–8.
6. Barrow DA, Petroff TE, Tandon RP, Sayer M. Characterization of thick lead zirconate titanate films fabricated using a new sol gel based process. *J Appl Phys* 1997;**81**:876–81.
7. Corker DL, Zhang Q, Whatmore RW, Perrin C. PZT 'composite' ferroelectric thick films. *J Eur Ceram Soc* 2002;**22**:383–90.
8. Livage J, Henry M, Sanchez C. Sol–gel chemistry of transition metal oxides. *Prog Solid State Chem* 1988;**18**:259–341.
9. Brinker CJ, Scherrer GW. *Sol–gel science: the physics and chemistry of sol–gel processing*. Boston: Academic Press; 1990.
10. Oliver WC, Pharr GM. An improved technique for determining hardness and elastic modulus using load and displacement sensing indentation experiments. *J Mater Res* 1992;**7**:1564–83.
11. Brinker CJ, Hurd AJ. Fundamentals of sol–gel dip-coating. *J Phys III France* 1994;**4**:1231–42.
12. Phalippou J. From gel to glass. *CR Chim* 2002;**5**:855–63.
13. Petit F, Vandeneede V, Cambier F. Relevance of instrumented microindentation for the assessment of hardness and Young's modulus of brittle materials. *Mater Sic Eng A* 2007;**456**:252–60.
14. Attunes JM, Cavalier A, Meekness LF, Simons MI, Fernandez JV. Ultramicrohardness testing procedure with Vickers indenter. *Surf Coat Technol* 2002;**149**:27–35.